Circuital and Numerical Models for Calculation of Shielding Effectiveness of Enclosure with Apertures and Monitoring Dipole Antenna Inside

Vesna MILUTINOVIĆ[1], Tatjana CVETKOVIĆ[1], Nebojša DONČOV[2], Bratislav MILOVANOVIĆ[2]

[1] Republic Agency for Electronic Communications, Višnjićeva 8, 11000 Belgrade, Serbia
[2] Faculty of Electronic Engineering, University of Niš, Aleksandra Medvedeva 14, 18000 Niš, Serbia

vesna.milutinovic@ratel.rs, tatjana.cvetkovic@ratel.rs, nebojsa.doncov@elfak.ni.ac.rs,
bratislav.milovanovic@elfak.ni.ac.rs.

Abstract. *In this paper, circuital and numerical models of metal enclosure with apertures are considered for the purpose of accurate shielding effectiveness calculation. An improved circuital model is presented to account for the presence of receiving dipole antenna which is often used in practice to measure the level of electromagnetic field at selected points inside the enclosure. Receiving antenna of finite dimensions could significantly change the EM field distribution inside the enclosure and thus affect the results for SE. TLM method incorporating wire node is used to create a numerical model. Both models are compared in terms of their ability to account for receiving antenna impact on shielding effectiveness of rectangular enclosure with aperture. In addition, comparison of both models is carried out for the case when an array of apertures with different aperture separation is present on one of the enclosure walls whereby the numerical TLM model is additionally enhanced with compact air-vent model.*

Keywords

Enclosure, shielding properties, plane wave, apertures, dipole antenna, circuital model, numerical TLM model.

1. Introduction

From the viewpoint of electromagnetic compatibility (EMC), performances of electronic systems enclosed in enclosures, dominantly depend on the nature and existence of interconnecting paths. Shielded enclosures have a major role in eliminating or reducing these interconnecting paths which cause coupling between electromagnetic (EM) energy sources and sensitive electronic systems. Wired and dielectric structures within the electronic system have also EM radiation excitation characteristics. The material and construction of the enclosure determine its properties as a shield which acts as a barrier to the level of EM radiation from the environment that reaches the electronic equipment, but also determines how much energy is radiated by the electronic equipment into the environment. Enclosure protects system components against externally or internally generated interference, but often they have a number of apertures with different size and patterns, used for airing, heat dissipation, control panels, outgoing or incoming cable penetration or other purposes, that can compromise its shield role. Therefore, it is very important to estimate shielding properties of enclosure in the presence of apertures.

One way of expressing shielding properties of enclosure is to calculate its shielding effectiveness (SE) which is defined as a ratio of EM field strength at some point in the presence and absence of enclosure. A wide range of techniques are currently available for the calculation of the SE, from analytical methods to numerical simulations. Some analytical methods were proposed in [1], [2], while in addition the solution in [2] was enhanced in [3] to allow for considering oblique incidence and polarization of incident plane wave and arbitrary location of apertures in relation to plane wave propagation. The numerical methods were also used for the SE calculation such as the finite-difference time domain (FDTD) method in [4], the methods of moments (MoM) in [5] and the transmission line matrix (TLM) method in [6]. Regarding the application of differential numerical methods in the time-domain, FDTD and TLM, conventional approach based on fine mesh description of fine features such as slots and apertures, was used in [4] and [6]. Authors of this paper have conducted, in parallel with research presented in [5], their own analysis how various factors, such as aperture patterns, their dimensions, number and orientation with the respect of enclosure walls or plane wave propagation direction, influence on the SE of enclosure. The results of this analysis have been presented in [7], [8]. In addition, an impact of plane wave excitation parameters on shielding properties of enclosure with multiple apertures has been considered by the authors in [9], [10]. In [7-10], a conventional TLM method was also used as in [5] to numerically study these various effects at high frequencies.

Aim of this paper is to investigate an impact of a small dipole antenna, often used in an experimental setup to measure the level of EM field at some characteristic

points in the enclosure, on the SE of enclosure. Other antennas are also used for measurement of shielding efficiency such as a spiral antenna presented in [11]. Antenna of finite dimensions could significantly affect the EM field distribution in closed environment as already experimentally shown in [12] for resonant cavity based microwave applicators. In a metal enclosure, this effect on the results of SE is numerically illustrated in [13]. In order to consider this impact on detected EM field level during the experimental SE characterization and determine the real SE of shielding enclosure, the existing analytical/circuital model presented in [3] is improved in this paper to include dipole antenna presence. Circuital model in [3] was developed to efficiently calculate the SE of enclosure for oblique incident plane wave of arbitrary polarization and for arbitrary location of apertures with respect of plane wave propagation but did not take into account the presence of receiving antenna. This model limitation was mentioned in [3] as one of possible causes for some differences between model and experimental SE results. The TLM method, incorporating compact wire model presented in [14], is also used here as in [13] to create a numerical model capable to take into account the antenna presence and position and their impact on the SE of enclosure. In addition, both models are compared for the case when an array of apertures with different aperture separation is present on one of the enclosure walls whereby the numerical model is additionally enhanced with compact air-vent model presented in [15], [16].

2. Incorporation of Monitoring Antenna into Circuital Model

In analytical/circuital model [3], it was proposed that the SE of enclosure with apertures on one or multiple sides can be simply calculated by superposition of one-dimensional results and that the problem of SE can be solved considering the field with arbitrary incidence and polarization angle, by virtue of vector decomposition.

The electric field E can be decomposed into x-, y- and z-components by simple vector analysis [3]:

$$E = \hat{x}\left(-\cos\phi\cos\theta\cos\psi - \sin\phi\sin\psi\right)E_0 + \hat{y}\left(-\sin\phi\cos\theta\cos\psi + \cos\phi\sin\psi\right)E_0 + \hat{z}\left(\sin\theta\cos\psi\right)E_0 \quad (1)$$

where E_0 is the magnitude of E. In this equation, the constants of E are defined as factors of polarization F_{px}, F_{py} and F_{pz}, which used for calculating SE. In this paper we will only consider the case of plane wave excitation with vertical polarization (along the z-axis) so that $E = \hat{z}E_0$.

The propagation vector $\boldsymbol{\beta}$ is also given as [3]:

$$\beta = \hat{x}\left(-\cos\phi\sin\theta\right)\beta_0 + \hat{y}\left(-\sin\phi\sin\theta\right)\beta_0 + \hat{z}\left(-\cos\theta\right)\beta_0 \quad (2)$$

where β_0 is the magnitude of the propagation vector, and the constants of β are defined as factors of incidence F_{ix}, F_{iy} and F_{iz} for each direction. For the case of normal incidence (propagation along the x-axis), as shown in Fig. 1a, $\beta = -\hat{x}\beta_0$.

Field intensity for appropriate mode at an arbitrary position in an enclosure can be calculated by using the mode factor F_m defined in [3]. In the circuital model shown in Fig. 1b, the enclosure is presented as a shorted rectangular waveguide in which the propagation is along the x-axis whose characteristic impedance and propagation constant are Z_{gx} and k_{gx}, respectively. The radiating source is represented by voltage v_0 and impedance $Z_0 = 377\ \Omega$. One aperture on enclosure wall is represented as a coplanar strip transmission line of length l_{ap} and with characteristic impedance Z_{0s} and phase constant k_0. Transforming the short circuits at both ends to the center of aperture, as shown in [2], the impedance of one aperture Z_{ap} can be obtained. The total impedance representing the n apertures on yz-plane enclosure wall normal to the plane wave propagation, Z_{apx}, is calculated by simply multiplying impedance Z_{ap} with n. Expressions for all variables used in the circuital model can be found in [2], [3].
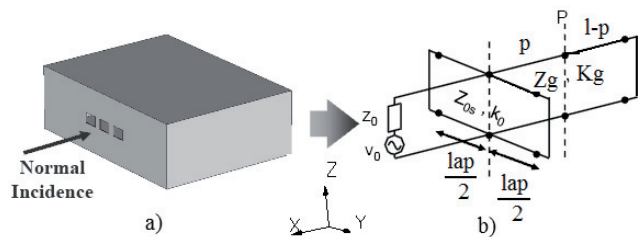
Fig. 1. a) Rectangular enclosure with apertures on the front wall, excited by normal incident plane wave with vertical polarization and b) circuital model of enclosure [3].

Calculation of the electric field inside the enclosure at distance p_x from the wall with aperture is transformed to the calculation of voltage v_{px} in the equivalent circuit [2] (see Fig. 2):

$$v_{1x} = v_0 \frac{Z_{apx}}{Z_0 + Z_{apx}}, \quad (3)$$

$$z_{1x} = \frac{Z_0\ Z_{apx}}{Z_0 + Z_{apx}}, \quad (4)$$

$$v_{2x} = \frac{v_{1x}}{\cos\left(k_{gx}p_x\right) + jZ_{1x}\sin\left(k_{gx}p_x\right)/Z_{gx}}, \quad (5)$$

$$Z_{2x} = \frac{Z_{1x} + jZ_{gx}\tan\left(k_{gx}p_x\right)}{1 + jZ_{1x}\tan\left(k_{gx}p_x\right)/Z_{gx}}, \quad (6)$$

$$Z_{3x} = jZ_{gx}\tan\left[k_{gx}\left(l_x - p_x\right)\right]. \quad (7)$$

In order to include the presence of receiving antenna, we introduce the impedance of antenna, Z_{ant}, at observing

point P in the equivalent circuital model. The input impedance of dipole antenna is obtained numerically by using the software package WIPL-D [17] for the case of 100 mm long wire oriented along z-axis (to detect vertically polarized E field) and placed inside the rectangular enclosure of the dimensions 300 mm x 400 mm x 200 mm. The set of numerical calculation were performed to account for different wire radius impact on its input impedance. As an illustration, the input impedance of dipole antenna, consisting of radiation resistance (real part) and reactance (imaginary part), represented as 100 mm long wire having radius of 0.08 mm is shown in Fig. 3.
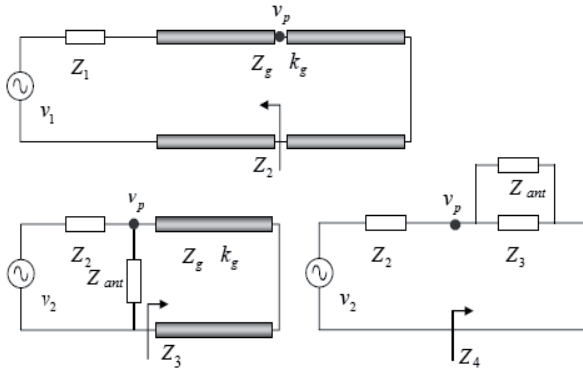

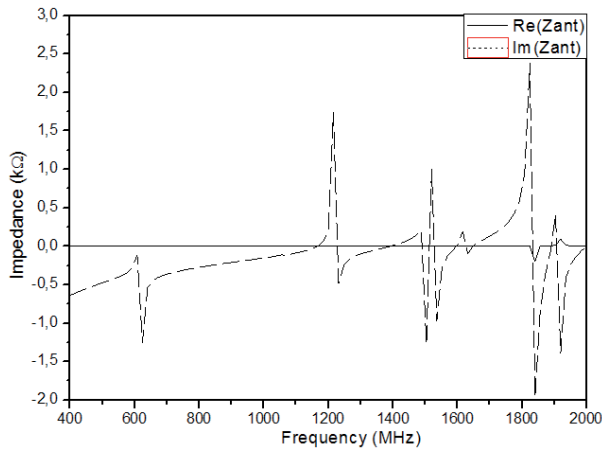**Fig. 2.** Voltage calculation at the observing point P that includes the presence of receiving antenna.

Fig. 3. Impedance of vertical antenna obtained by WIPL-D.

In circuital model, the impedance Z_{4x} is then:

$$Z_{4x} = \frac{Z_{3x} \, Z_{ant}}{Z_{3x} + Z_{ant}} . \qquad (8)$$

From this equation, the voltage at observing point P in the presence of enclosure can be calculated is:

$$v_{px} = v_{2x} \frac{Z_{4x}}{Z_{2x} + Z_{4x}} \qquad (9)$$

and in the absence of enclosure as:

$$v_p = v_0 / 2 . \qquad (10)$$

SE for plane wave propagating in x-direction and

with z-polarization, se_{zx}, at point P inside enclosure is defined as follows:

$$se_{zx} = F_m \frac{2v_{px}}{v_0} . \qquad (11)$$

We can get the total se_{zx} by summing of se_{zx} for (n, l) modes, which are function of n and l, and by multiplying factor of polarization F_{pz} and factor of incidence F_{ix}. The total se_{zx} is given by:

$$se_{zx}^{total} = F_{pz}F_{ix}\sum_{n}\sum_{l} se_{zx}(n,l), \qquad (12)$$

$$se_z = \left| se_{zx}^{total} \right| , \qquad (13)$$

$$SE_z = -20\log_{10}\left| se_z \right| . \qquad (14)$$

3. Numerical Model

3.1 Compact TLM Wire Model

The TLM method [18] is a numerical modeling technique based on temporal and spatial sampling of EM fields. In TLM method, a three-dimensional (3D) EM field distribution is modeled by filling the space with a network of transmission link lines and exciting a particular field component in the mesh. EM properties of a medium are modeled by using a network of interconnected nodes. A typical node structure is the symmetrical condensed node (SCN), which is shown in Fig. 4. Additional stubs can be attached to SCN to model inhomogeneous and lossy materials.
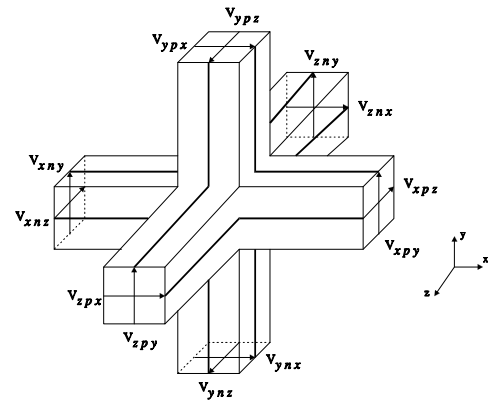

Fig. 4. Symmetrical condensed node.

Compact TLM wire model, which allows for accurate modeling of wires with a considerably smaller diameter than the node size, has been introduced in [14]. It uses a special wire network formed by using additional link and stub lines (Fig. 5) whose characteristic impedance parameters, Z_w and Z_{ws}, are chosen to model the capacitance and inductance increased by the wire presence, while at the same time maintaining synchronism with the rest of the transmission line network. This wire network is embedded within the TLM nodes to model signal propagation along

the wires, while allowing for interaction with the EM field (Fig. 6). Coupling between the additional link and stub lines with the rest of TLM node is achieved through points *A* and *B*.
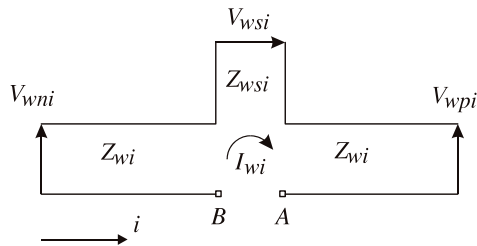

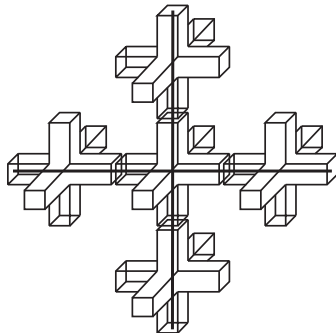**Fig. 5.** Wire network for a wire running in *i*-direction.

Fig. 6. Wire network embedded within the TLM nodes.

The single column of TLM nodes, through which wire conductor passes, can be used to approximately form the fictitious cylinder which represents capacitance and inductance of wire per unit length. Its effective diameter, different for capacitance and inductance, can be expressed as a product of factors empirically obtained by using known characteristics of TLM network and the mean dimensions of the node cross-section in the wire running direction [14].

3.2 Compact TLM Air Vent Model

To accurately capture the strong variation of EM fields inside and around the array of apertures (so-called air vents present on enclosure walls due to ventilation purposes) by conventional TLM approach, several computational nodes are normally needed across each aperture dimension and across the depth of the supporting panel. Including these small details in an otherwise large modeling space can be computationally very expensive. Therefore, in [15] a compact TLM air-vent model, in the form of equivalent LC circuit (Fig. 7), embedded into an otherwise coarse TLM mesh, has been proposed to accurately and efficiently account for EM presence of apertures. Empirically found capacitance and inductance of equivalent circuit for each polarization are implemented in conventional TLM mesh using additional short- and open-circuit stabs at the interface between two TLM nodes (Fig. 8). In [16], the model has been extended to account for rectangular and hexagonal apertures besides square and circular apertures

considered in [15]. Air-vent model is limited to frequencies at which apertures are closer than a half wavelength apart and where there are no structures within the evanescent field beyond apertures.
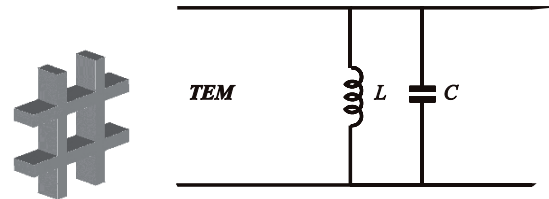

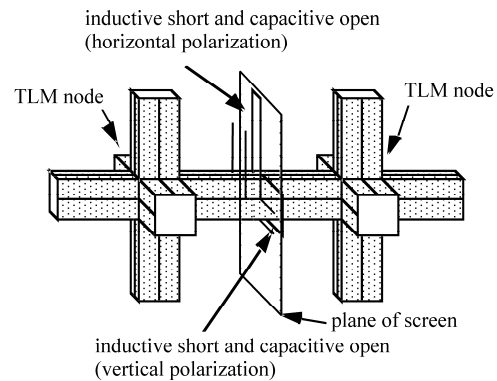**Fig. 7.** Compact air-vent model based on LC network.

Fig. 8. Implemented LC model at the interface between two TLM nodes.

4. Results

A rectangular metal enclosure, with dimensions 300 mm x 400 mm x 200 mm (Fig. 9a) is considered in this paper for circuital and numerical models calculation of the SE. One rectangular aperture of dimensions *l* x 2*s* = 50 mm x 30 mm exists on the front enclosure wall of thickness 0.2 mm in zy-plane (Fig. 9b). The aperture is symmetrically placed around the center of the front wall. A plane wave of normal incidence to the frontal panel and with vertical electric polarization is used as an excitation. The dipole antenna of length 100 mm, oriented along z-axis, is used to measure the level of EM field inside the enclosure. Choice of geometry and dimensions of the enclosure and aperture, type of excitation, location of the antenna (5 mm off the enclosure center in x-direction) and its length were governed by experimental arrangements presented in [3]. It should be noted that in [3] the radius of the receiving antenna used in the measurements is not specified as well as characteristics of balun placed between antenna and cable to enhance the antenna efficiency.

First, the influence of dipole antenna on EM field inside the enclosure is analyzed by using the proposed modified circuital model. It is assumed that the radius of the wire used to represent dipole antenna is 0.08 mm. As previously said, WIPL-D software is used to calculate the input impedance of the considered radius of the wire. Circuital model result for SE, obtained for rectangular aper-

ture 50 mm x 30 mm on the front wall and for the cases when dipole antenna is excluded from and included in equivalent circuit model, are compared with measurements results [3] and shown in Fig. 10.
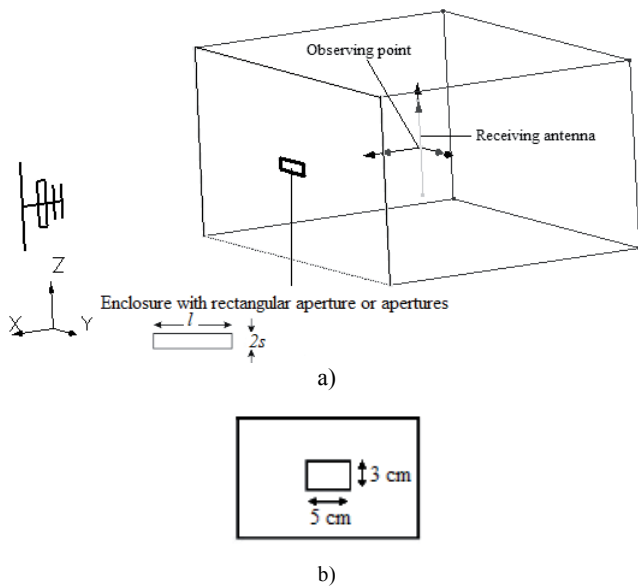

Fig. 9. a) Rectangular metal enclosure with rectangular aperture on the front wall excited by normal incidence plane wave with vertical polarization, b) frontal panel with one rectangular aperture.
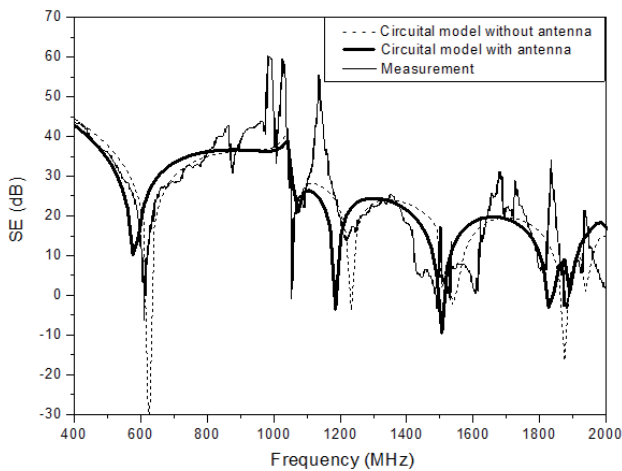

Fig. 10. SE$_z$ of metal enclosure with rectangular aperture 50 mm x 30 mm on the front wall - circuital model and measurements [3].

It can be seen that in both cases (without and with the antenna) the circuital model results follow fairly well the experimental results curve. There is a relatively small difference between the levels of SE for these two cases which can be explained that the considered antenna is very thin. Also, resonant frequencies, when antenna is included in the circuital model, are shifted towards lower frequencies. The similar conclusions can be derived for other two aperture patterns (one rectangular aperture of dimensions lx$2s$ = 50 mm x 10 mm and three rectangular apertures of dimensions lx$2s$ = 50 mm x 10 mm on the frontal wall) considered in [3].

The difference between the measured level of SE (SEmeas) and the level of SE obtained by the circuital model without antenna (SE$_1$) and with antenna (SE$_2$) is shown in Tab. 1. The average value of difference between measured and circuital model results given in Tab. 1 is around 5.5 dB in the considered frequency range.

f (MHz)	SEmeas. (dB)	SE$_1$ (dB)	SE$_2$ (dB)	|SEmeas-SE$_1$| (dB)	|SEmeas-SE$_2$| (dB)
400	43.51	44.58	42.98	1.07	0.53
500	35.92	37.8	34.41	1.88	1.51
600	12.02	21.62	22.5	9.60	10.48
700	28.47	30.51	33.72	2.04	5.25
800	36.06	35.1	36.29	0.96	0.23
900	38.51	36.48	36.7	2.03	1.81
1000	45.79	37.72	36.69	8.07	9.10
1100	28.19	28.19	26.51	0.00	1.68
1200	19.33	21.05	15.2	1.72	4.13
1300	22.43	23.36	24.5	0.93	2.07
1400	18.21	23.18	20.88	4.97	2.67
1500	17.65	2.12	-9.25	15.53	26.90
1600	1.76	15.65	18.68	13.89	16.92
1700	22	19.65	19.3	2.35	2.70
1800	6.84	15.83	9.67	8.99	2.83
1900	5.34	9.05	8.41	3.71	3.07
2000	2.19	14.9	16.85	12.71	14.66

Tab. 1. Comparison between measured level of SE (SEmeas.) and the level of SE obtained from the circuital model when antenna is excluded (SE$_1$) and included (SE$_2$).

Impact of antenna radius on the SE of enclosure, investigated by using the improved circuital model, is shown in Fig. 11 for one rectangular aperture 50 mm x 30 mm on the frontal wall. As it can be seen from Fig. 11, when wire radius is decreasing resonant frequencies are approaching to the case when antenna is excluded from the circuital model. Around these resonant frequencies the level of SE is very small so one should take into account this resonant frequency shift due to antenna presence during the experimental SE measurement. For example at the first resonant frequency there is a difference of approximately 15 dB between the SE results obtained by circuital model with antenna of radius 0.08 mm and antenna with 20 times greater radius (1.6 mm). The difference between the locations of the first resonant frequency for these two radii is around 48 MHz.

Coaxial cable is often used to carry out the induced signal on the dipole antenna to the network analyzer in order to measure the EM field level. The influence of coaxial cable impedance Z_p, added to the input impedance of monitoring dipole antenna of radius 1.6 mm, is illustrated in Fig. 12 for the case of rectangular aperture 50 mm x 30 mm on the front enclosure wall. It can be seen that at

the resonant frequencies the SE has a higher value when greater cable impedance is used and that in the rest of frequency range the SE curves are overlapping.
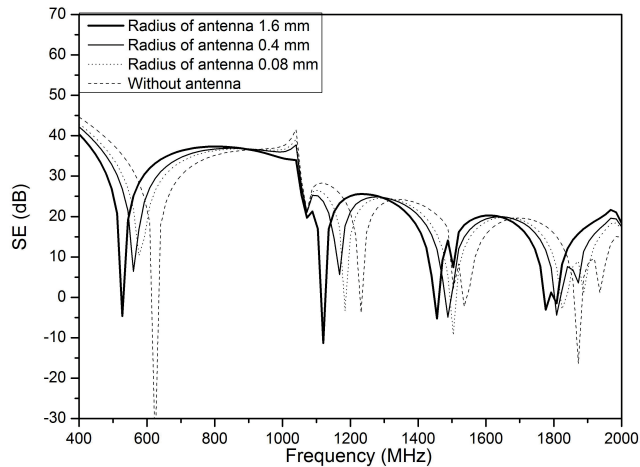
Fig. 11. Circuital model results for SE_z of metal enclosure with rectangular aperture 50 mm x 30 mm on the front wall: different values of wire radius.
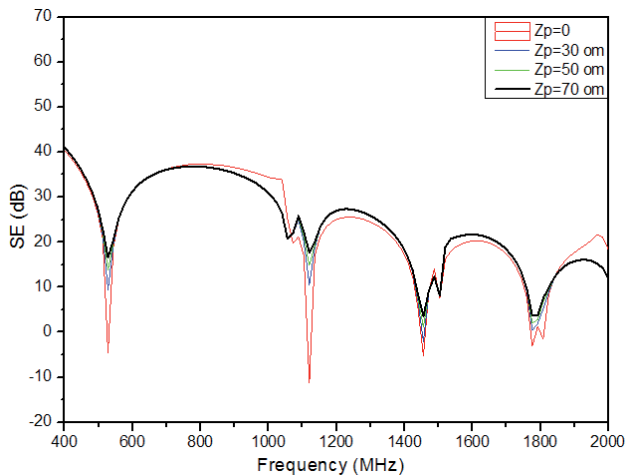
Fig. 12. Circuital model results for SE_z of metal enclosure with rectangular aperture 50 mm x 30 mm on the front wall: different values of coaxial cable impedance.
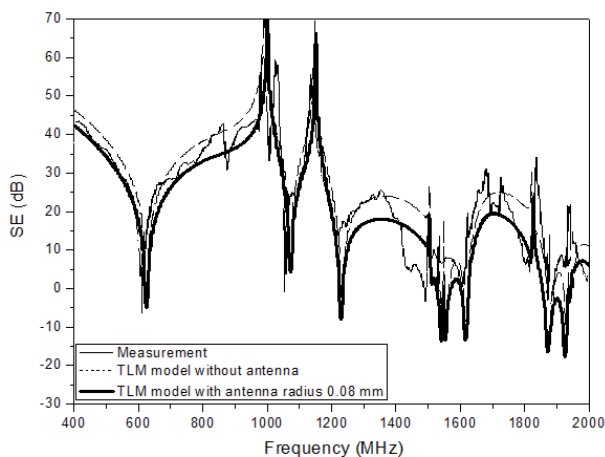
Fig. 13. SE_z of metal enclosure with rectangular aperture 50 mm x 30 mm on the front wall - numerical TLM model and measurements [3].

Numerical model, incorporating the compact TLM wire description of dipole antenna, is also used to calculate the SE of considered enclosure. The receiving antenna is represented as z-directed 100 mm long wire having the radius of 0.08 mm. Its position within the enclosure is the same as in previous cases. SE results, obtained by numerical TLM models without and with antenna, for one aperture 50 mm x 30 mm on the front wall, are shown in Fig. 13 together with measurement results [3].

It can be seen that numerical TLM model without and with antenna provides the results that follow the experimental results curve better than the circuital model. Impact of antenna presence on the SE in comparison with the case when the antenna is excluded from the numerical model can be also observed. The difference between the measured level of SE (SEmeas) and the level of SE obtained by TLM model without (SE_1) and with (SE_2) antenna in considered frequency range is given in Tab. 2.

f (MHz)	SEmeas. (dB)	SE_1 (dB)	SE_2 (dB)	|SEmeas-SE_1| (dB)	|SEmeas-SE_2| (dB)
400	43.51	46.53	42.38	3.02	1.13
500	35.92	38.4	34.14	2.48	1.78
600	12.02	22.55	18.24	10.53	6.22
700	28.47	30.7	26.1	2.23	2.37
800	36.06	38.26	33.05	2.20	3.01
900	38.51	42.52	36.45	4.01	2.06
1000	45.79	56.13	67.1	10.34	21.31
1100	28.19	31.9	25.92	3.71	2.27
1200	19.33	26.21	19.3	6.88	0.03
1300	22.43	22.28	16.95	0.15	5.48
1400	18.21	23.58	17.35	5.37	0.86
1500	17.65	18.46	11.06	0.81	6.59
1600	1.76	5.84	0.6	4.08	1.16
1700	22	24.66	19.53	2.66	2.47
1800	6.84	21.33	12.23	14.49	5.39
1900	5.34	3.65	-2.66	1.69	8.00
2000	2.19	10.85	5.9	8.66	3.71

Tab. 2. Comparison between the measured level of SE (SEmeas.) and the level of SE obtained from TLM model when the antenna is excluded (SE_1) and included (SE_2).

Due to some uncertainties of measurements conducted in [3] (such as radius of the dipole-receiving antenna) and having in mind that the compact wire model is already numerically [14] and experimentally verified [12], authors focus their attention on the effect of wire presence inside the enclosure. Fig. 14 shows that the SE with the receiving antenna placed in enclosure has a constant lower value across the considered frequency range than the curve for the SE obtained without receiving antenna. This drop in the SE level is bigger than one obtained by cir-

cuital model and it can be explained due to nature of numerical model to account for two-ways interactions between antenna and EM field, i.e. induced wire current causes that wire behaves as a second emitter and it has a return influence on EM field inside the enclosure. Resonant frequencies shift towards lower frequencies when radius of the antenna is increasing can be also observed but this shift is significantly smaller than one obtained by the circuital model. Numerical model is capable to explicitly account for dependence of wire capacitance and inductance per unit length on radius [14], [18], while the circuital model contains only simplified impedance representation of the dipole antenna, obtained numerically by WIPL-D, in the equivalent circuit. For example, at the first resonant frequency there is a difference of approximately 4.6 dB between the SE results obtained by numerical model with antenna of radius 0.08 mm and antenna with 20 times greater radius (1.6 mm). The difference between the locations of the first resonant frequency for these two radii is around 1.8 MHz.
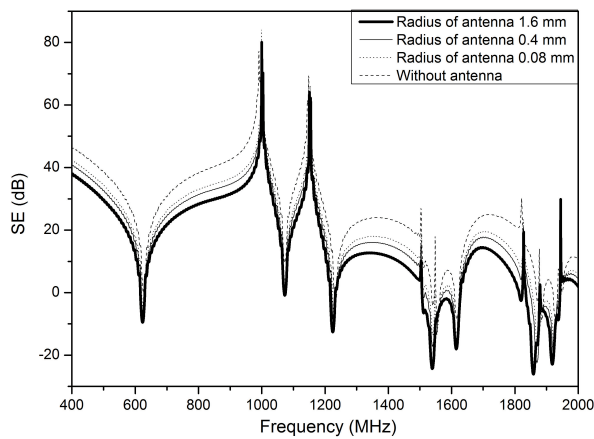

Fig. 14. Numerical model results for SE_z of metal enclosure with rectangular aperture 50 mm x 30 mm on the front wall - different values of wire radius.

Finally, circuital and numerical models are compared in terms of their ability to account for different number of so-called air-vent apertures with different aperture separation on enclosure wall. Numerical model is additionally enhanced with compact air-vent model presented in subsection 3.2. The results for the SE obtained by both models for (4x2) array of square apertures with length of 7.9 mm (Fig. 15) and different aperture separation expressed through wavelength corresponding to the maximum frequency of interest are shown in Figs. 16-18. The dipole antenna is not included in both models. SE results obtained by conventional TLM approach, where fine mesh is used to describe cross-section of apertures and their mutual distance instead of compact air-vent model, are shown in the same figure.

It can be seen that, except for the case when aperture separation is equal to half wavelength, fine TLM mesh results are in good agreement with the results obtained by numerical model enhanced with compact air-vent model.

The case shown in Fig. 16 is at the limit of applicability of air-vent model. Also, circuital model highly underestimates the SE of enclosure due to its incapability to take into account the mutual separation between apertures.
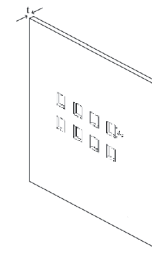

Fig. 15. (4x2) array of square apertures with length of 7.9 mm on the front enclosure wall.
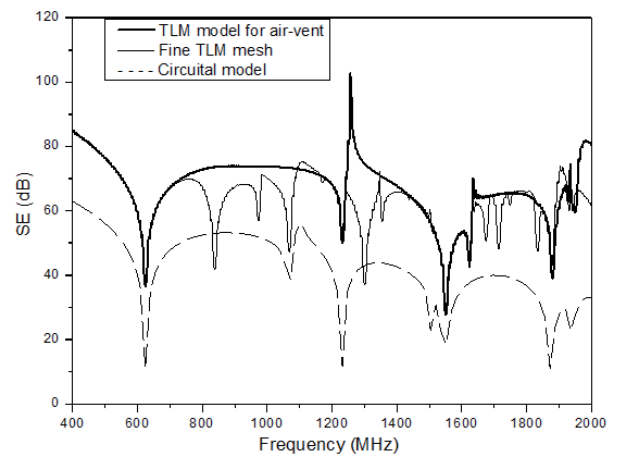

Fig. 16. SE_z of metal enclosure without antenna and with (4x2) array of square apertures with length of 7.9 mm and $\lambda/2$ separation between apertures.
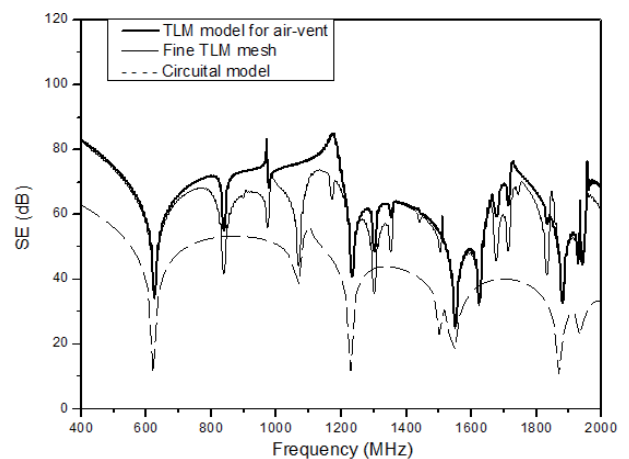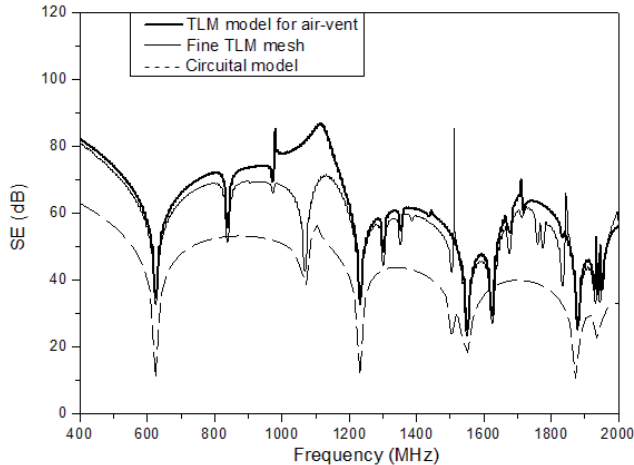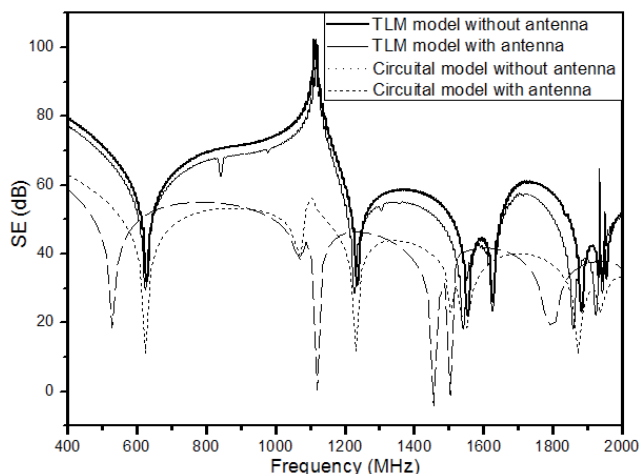

Fig. 17. SE_z of metal enclosure without antenna and with (4x2) array of square apertures with length of 7.9 mm and $\lambda/4$ separation between apertures.

Results for the SE of enclosure for (4x2) array of square apertures with length of 7.9 mm and 2.1 mm aperture separation obtained by circuital and numerical models that take into account the presence of antenna with radius of 1.6 mm are shown in Fig. 19. Again the same effects of antenna presence on the SE curves can be observed. As it

can be seen, the antenna presence has a considerable impact on EM field level inside the enclosure. Results obtained using circuital model are lower than numerical results. The difference between SE of enclosure, obtained by both models, also becomes more evident as frequency decreases, especially around the first resonant frequency.

Fig. 18. SE_z of metal enclosure without antenna and with (4x2) array of square apertures with length of 7.9 mm and $\lambda/16$ separation between apertures.

Fig. 19. SE_z of metal enclosure with and without antenna and with (4x2) array of square apertures with length of 7.9 mm and 2.1 mm separation between apertures.

5. Conclusions

An impact of a small dipole antenna, used to measure the level of EM field at some characteristic points in the enclosure, on the SE of the enclosure is investigated in this paper. Two models, one based on the equivalent circuit and enhanced here to include the presence of EM field monitoring antenna and other based on TLM method with compact wire and air-vent models, have been used to accurately estimate the SE of the enclosure with apertures. Results from both models have demonstrated that the coupling due to the receiving antenna presence, inevitable in the meas-

urement process, can be very significant especially regarding the resonant frequencies locations and level of SE in considered frequency range. Therefore, this impact has to be taken into account during the experimental characterization in order to correctly estimate the SE of the metal enclosure. Circuital model is able to provide fast information about the level of SE, but its main limitations are due to considering only one-way interaction between EM field and the antenna and its incapability to take into account the mutual separation between apertures in the case of air-vents. Numerical TLM model is capable to accurately account for not just passive but also active presence of the dipole antenna inside the enclosure and for EM presence of air-vents including the distance between apertures, but it is slower to run even with implemented compact models for wires and air-vents. Future research will be focused to more strict comparisons of these two models in terms of their accuracy to account for not just antenna presence, but also physical and electrical presence of the cable connecting the dipole antenna to a measuring equipment and to derivation of a factor that should be added to the measured level of SE in order to compensate antenna and cable presence inside the enclosure.

Acknowledgements

References

[1] MENDEZ. H. A. Shielding theory of enclosures with apertures. *IEEE Transactions on Electromagnetic Compatibility,* 1978, vol. 20, no. 2, p. 296–305.

[2] ROBINSON, M. P., BENSON, T. M., CHRISTOPOULOS, C., DAWSO, J. F., GANLEY, M. D., MARVIN, A. C., PORTER, S. J., THOMAS, D. W. P. Analytical formulation for the shielding effectiveness of enclosures with apertures. *IEEE Transactions on Electromagnetic Compatibility*, 1998, vol. 40, no. 3, p. 240–248.

[3] SHIM, J., KAM, D. G., KWON, J. H., KIM, J. Circuital modelling and measurement of shielding effectiveness against oblique incident plane wave on apertures in multiple sides of rectangular enclosure. *IEEE Transactions on Electromagnetic Compatibility*, 2010, vol. 52, no. 3, p. 566–577.

[4] NUEBEL, L. J., DREWNIAK, J. L., DUBROFF, R. E., HUBING, T. H., VAN DOREN, T. P. EMI from cavity modes of shielding enclosures – FDTD modeling and measurements. *IEEE Transactions on Electromagnetic Compatibility*, 2000, vol. 42, no. 1, p. 29–38.

[5] ALI, S., WEILE, D. S., CLUPPER, T. Effect of near field radiators on the radiation leakage through perforated shields. *IEEE Transactions on Electromagnetic Compatibility*, 2005, vol. 47, no. 2, p. 367–373.

[6] NIE, B. L., DU, P. A., YU, Y. T., SHI, Z. Study of the shielding properties of enclosures with apertures at higher frequencies using

the transmission-line modeling method. *IEEE Transactions on Electromagnetic Compatibility*, 2011, vol. 53, no. 1, p. 73–81.

[7] MILOVANOVIĆ, B., DONČOV, N., MILUTINOVIĆ, V., CVET-KOVIĆ, T. Numerical characterization of EM coupling through the apertures in the shielding enclosure from the viewpoint of electromagnetic compatibility. *Telecommunications - Scientific Journal Published by the Republic Agency for Electronic Communications – RATEL*, 2010, no. 6, p. 73-82.

[8] MILUTINOVIĆ, V., CVETKOVIĆ, T., DONČOV, N., MILOVA-NOVIĆ, B. Analysis of the shielding effectiveness of enclosure with multiple circular apertures on adjacent walls. In *Proceedings of the International Conference on Information. Communication and Energy Systems and Technologies – ICEST*. Niš (Serbia), 2011, p. 685-688.

[9] CVETKOVIĆ, T., MILUTINOVIĆ, V., DONČOV, N., MILOVA-NOVIĆ, B. Analysis of the influence of polarization and direction of propagation of an incident plane wave on the effectiveness of rectangular enclosures with apertures. In *Proceedings of the INFOTEH Conference*. Jahorina (Bosnia and Herzegovina), 2011, vol. 10, Ref.B-I-6, p. 90-94.

[10] MILUTINOVIĆ, V., CVETKOVIĆ, T., DONČOV, N., MILOVA-NOVIĆ, B. Analysis of enclosure shielding properties dependence on aperture spacing and excitation parameters. In *Proc. of the IEEE TELSIKS Conf.*. Niš (Serbia), 2011, vol. 2, p. 521 to 524.

[11] KOŘÍNEK, T., PIKSA, P., MAZÁNEK, M. Wideband measurement in a small shielded box using equiangular spiral antennas. *Radioengineering*, 2006, vol. 15, no. 4, p. 34-37.

[12] JOKOVIĆ, J., MILOVANOVIĆ, B., DONČOV, N. Numerical model of transmission procedure in a cylindrical metallic cavity compared with measured results. *International Journal of RD and Microwave Computer-Aided Engineering*, 2008, vol. 18, no. 4, p. 295-302.

[13] MILUTINOVIĆ, V., CVETKOVIĆ, T., DONČOV, N., MILOVANOVIĆ, B. Shielding effectiveness of rectangular enclosure with apertures and real receiving antenna. In *Proceedings of the INFOTEH Conference*. Jahorina (Bosnia and Herzegovina), 2012. vol. 11, Ref.KST-4-9, p. 440-444.

[14] WLODARCZYK, A. J., TRENKIC, V., SCARAMUZZA, R., CHRISTOPOULOS, C. A fully integrated multiconductor model for TLM. *IEEE Transactions on Microwave Theory and Techniques,* 1998, vol. 46, no. 12, p. 2431-2437.

[15] DONCOV, N., WLODARCZYK, A. J., SCARAMUZZA, R., TRENKIC, V. Compact TLM model for air-vents. *Electronics Letters*, 2002, vol. 38, no. 16, p. 887-889.

[16] DONCOV, N., MILOVANOVIC, B., STANKOVIC, Z. Extension of compact TLM air-vent model on rectangular and hexagonal apertures. *Applied Computational Electromagnetics Society (ACES) Journal*, 2011, vol. 26, no.1, p. 64-72.

[17] WIPL-D Pro v10.0. WIPL-D Team. [Online] Available at: http://www.wipl-d.com.

[18] CHRISTOPOULOS, C. *The transmission-Line Modelling (TLM) Method*. Piscataway, NJ: IEEE Press in association with Oxford University Press, 1995.

About Authors …

Vesna MILUTINOVIĆ graduated in 2000 at the Faculty of Electronics in Nis, at the Department of Electronics and Telecommunications. Doctoral studies at the Faculty of Electronics in Nis, Department of Telecommunications, under the supervision of prof. Bratislav Milovanovic enrolled in October 2008. She has worked in planning, development and design of telecommunication networks. Since April 2007 she has been employed in RATEL for activities related to the control of radio communications. The author works in the field of telecommunication networks and systems.

Tatjana CVETKOVIĆ graduated in 1989 at the Military-Technical Faculty in Zagreb. Croatia, at the Department of Electronics and Telecommunications. Doctoral studies at the University of Niš, Faculty of Electronics, Department of Telecommunications, enrolled in 2008. She is employed in the Republic Agency for Electronic Communications, for activities related to the regulations in the area of electronic communications. She is an author and co-author of many conference works in the field of analyzing and calculation of shielding effectiveness of metal enclosures, and also in fields of regulation, realization and quality of electronic communication services.

Nebojsa DONČOV is an Associate Professor of Telecommunications at the University of Niš, Faculty of Electronic Engineering, Serbia. He received his PhD in Telecommunications from the University of Niš in 2002 and a Dipl.-Ing. Degree in Electronics and Telecommunications from the University of Niš in 1995. His current research focuses on computational and applied electromagnetics with a particular emphasis on TLM and network methods applications in microwaves and EMC.

Bratislav MILOVANOVIĆ received the Dipl.-Ing., MSc. and PhD degrees from the University of Niš, Serbia, in 1972, 1975 and 1979, respectively. He was promoted in full Professor in 1990. He was the Dean of the Faculty of Electronic Engineering from 1994–1998. His research interests include microwaves, computational electromagnetics and neural networks. He has published over 500 scientific papers in scientific journals and conference proceedings. He is general chairman of the TELSIKS conference, a full member of the Academy of Engineering Sciences of Serbia, a president of the National MTT Society and president of the IEEE MTT Chapter of Serbia and Montenegro.